Chapter 12
Indirect Matrix Converter for Distributed Generation Application: An Experimental Study

Rahul Kumar Garg, Kavita Yadav, Vinod Kumar and Monika Vardia

12.1 Introduction

Because of increasing demand of electrical energy and environmental concerns, wind power has become the most promising renewable resource. In spite of its tremendous growth, the wind power industry keeps moving forward in order to increase the production, efficiency, and controllability of the wind turbines along with its easiness for the integration with power grid. Also, it is environment friendly in the sense that for every 1 kWh of electricity generated by wind, the emission of CO_2 is reduced by 1 kg, and operation of a wind turbine (WT) weighing 50 tons prevents burning of 500 tons of coal annually.

As per reports of REN21 Renewables report, 2015, and WWEA report, 2015, the wind power has grown very fast to a capacity of 428 GW in 2015 and it is expected to achieve 760 GW in 2020.

The wind power can be harnessed by a WECS which has components such as WT, an electric generator, a power electronic converter, and the corresponding control system. Based on the types of components used, different WECS topologies can be realized. However, the objective in all topologies is the same, i.e., the wind energy as the conversion of varying wind velocities into electric power at the grid frequency [1–3].

Variable speed operation of wind turbines is desirable for wind energy conversion system (WECS) as it yields 10–15% more output energy with less WT costs. Among various variable speed WECS configurations, the doubly fed

R.K. Garg · K. Yadav · V. Kumar (✉)
Department of Electrical Engineering, Maharana Pratap University
of Agriculture and Technology, Udaipur, India
e-mail: vinodcte@yahoo.co.in

M. Vardia
Faculty of Engineering, Pacific Academy of Higher Education
and Research University, Udaipur, India

induction generator (DFIG)-based topology has been the dominant technology in the market since late 1990s [4]. However, with the development in trends of WECS toward larger power capacity, increased power density, lower cost per kW, and the need for higher reliability, this situation has changed in the last few years. Moreover, DFIG requires gearbox to match the rotor and turbine, which many times suffers from faults and requires regular maintenance, making the system unreliable.

Therefore, nowadays, more attention has been paid to direct-drive gearless WECS concepts, for which the permanent magnet synchronous generator (PMSG) has been found to be superior owing to its various advantages such as self-excitation capability leading to a higher power factor (pf) and higher efficiency operation, lower maintenance costs, higher precision, higher power density, better grid compatibility, better voltage, and power capabilities with simple control method, except initial installation costs [5–7]. But due to the advanced research made in the field of permanent magnet materials fabrication, it has extended the PMSG lifetime with decreased production cost. Also, with the modern use of sensorless control will further enhance the robustness and reliability, while reducing the cost and complexity of the WECS. Many WT manufacturers such as Siemens Wind Power, Goldwind, GE Energy, and Vestas have adopted the direct-drive PMSG concept in their WECS production.

The power semiconductor devices being the backbone of power electronics converter used for WECS determine many critical performances such as reliability, cost, and efficiency. Module-packaged IGBT, press-pack-packaged IGBT, and the press-pack packaging integrated gate commutated thyristor (IGCT) are the potential high-power silicon-based semiconductor technologies for WECS application. Recently, there is a booming development of silicon carbide (SiC)-based devices, which are majorly in the form of MOSFET as well as diodes. The module packaging technology of IGBT has good applications with fewer mounting restrictions, but because of the soldering and bond wire connection of internal chips, it suffers from larger thermal resistance, lower power density, and higher failure rates [8].

During the last 25 years, trends in power electronic technologies for wind power application have changed dramatically. In early 1980s, the power electronics for wind turbines was just a soft starter for interconnection of squirrel cage induction generator with the grid, whereas in 1990s, the diode bridges with chopper were used to control wound rotor induction generator. In 2000, AC/DC/AC converters known as back-to-back converters were introduced in large scale which started to regulate the generated power from turbines [9].

Presently, power electronics plays an important and decisive role in delivering electrical power from WECS based on PMSG directly to the grid or load. Generally, full-scale power electronic converters are commonly used to control and regulate the frequency and voltage amplitude of the generated electricity to meet the grid code requirements. Various power processing topologies have been proposed and investigated from time to time by different researchers. Conventionally, the AC/DC/AC conversion system was adopted for wind power applications, where GSC may be a diode rectifier cascaded with a boost converter by [10], PWM rectifier called as voltage-sourced converter (VSC) by [6, 6, 11–13], or a multilevel

converter by [9]. However, the grid side converter is often a VSC unit. Though AC/DC/AC converter has high energy density and is relatively low in price, has serious concerned as mentioned in [14–16] with its large dc link electrolytic capacitor which is a common cause for its premature failure. The other main shortcomings of the above-mentioned AC/DC/AC conversion units are (i) large physical dimensions, high weight, and excessive volume/footprint of the DC link component, i.e., the DC capacitor or the inductor, (ii) the low reliability of DC capacitor, (iii) the poor line pf and harmonic distortion in line and machine currents, (iv) poor device utilization, and (v) poor pf operation.

It is therefore required to remove the dc capacitor, which after all is the main attractiveness of the all semiconductor matrix converters which have high merits over AC/DC/AC converter such as improved voltage gain with simplified control, free from commutation problems, compact in size, light weight, high reliability due to the absence of dc capacitor, and providing extremely fast transient response [14, 17, 18]. Also, it is considered as an emerging alternative as it provides a large number of control levers that allow for independent control on the voltage, frequency, input pf, and phase angle. Recently, some work has been reported in the literature on matrix converter (MC)-based WECS using simulation environment [14, 17–19]. Based on the state of the art in WECS research discussed above, this chapter aims to experimentally investigate the MC-interfaced PMSG for WECS under different conditions, e.g., grid/load unbalance/balance and varying wind conditions.

12.2 Topology of Wind Energy Conversion System Under Investigation

Figure 12.1 shows the block diagram of the proposed unidirectional MC-interfaced PMSG-based WECS under investigation.
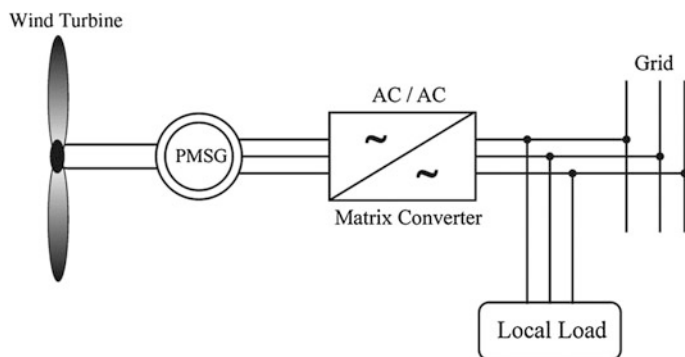

Fig. 12.1 Topology of wind energy conversion system under study

As it is shown in Fig. 12.1, MC is used for interfacing with the grid, and space vector PWM control is effectively used to achieve low-harmonic characteristics. It also performs pf control at grid interface and satisfies the reactive power demand. It implements the "perturbation and observation"-type MPPT scheme by controlling shaft speed to yield maximize energy output at varying wind speeds. A wind turbine emulator which drives the PMSG is developed for laboratory tests. Figure 12.2 presents the structure of the wind emulator. The wind speed changes, and load switching conditions are performed using the WT emulator, which consists of chopper dc drive, whose control is implemented using dSPACE DS1104 real time board.

It obtains the wind speed values, and by using the turbine characteristics and dc motor speed, it calculates the torque command of the WT. In this way, it is able to reproduce the steady and dynamic behavior of a real WT to the energy conversion system.

The schematic diagram of the unidirectional voltage-boosted MC with twelve switches (clamping circuit is not shown here) is shown in Fig. 12.3. It consists of
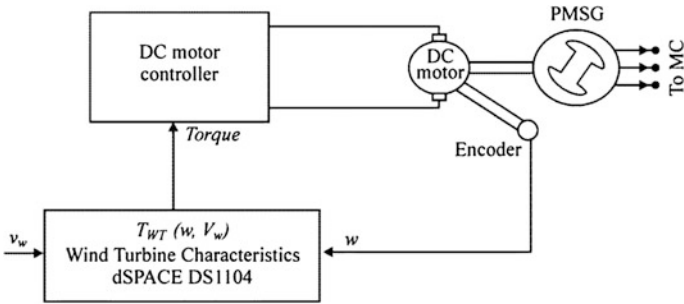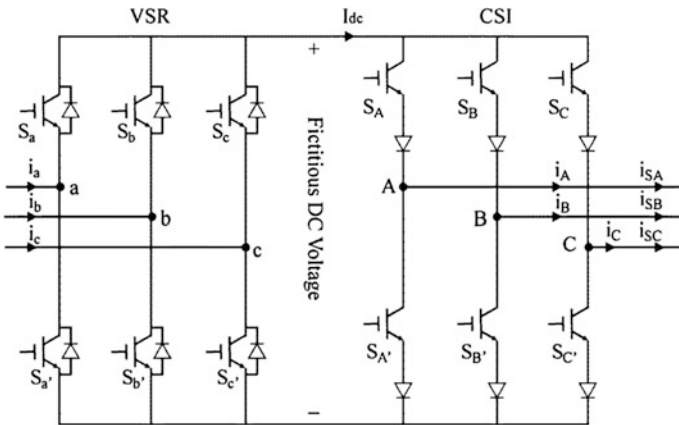
Fig. 12.2 Wind emulator system

Fig. 12.3 Schematic diagram of the voltage-boosted MC topology

six switches with antiparallel diodes that are arranged as front-end voltage source rectifier (VSR), whereas other six switches with series diodes as rear-end current source inverter (CSI) as explained in [14].

12.3 Novel Control Scheme

As we know that, at any given wind velocity, maximum power can be captured from the wind, if the shaft speed is adjusted at the value corresponding to the peak power. The novel idea is to change the angular frequency of PMSG through SVPWM control of voltage-boosted MC to track the shaft speed corresponding to the maximum turbine power at all times. The proposed MC incorporates perturbation & observation-type MPPT, which is a part of the adaptive fuzzy control system, which through the MC manages to yield maximum wind power according to the current wind speed by regulating the angular frequency of the PMSG. The value of ω_{ref} is dynamically approached in real time from fuzzy controller, using *P&O*-type MPPT. The algorithm can be explained as below:

$$\text{Pertubtaion} : \omega_{\text{ref}}(t) = \omega_{\text{ref}}(t-1) + s|\Delta\omega_{\text{ref}}| \tag{12.1}$$

$$\text{Observation} : \Delta P_0 = P_0(t) - P_0(t-1) \tag{12.2}$$

where

$\omega_{\text{ref}}(t)$	actual angular frequency sampling
$\omega_{\text{ref}}(t-1)$	previous angular frequency sampling
$|\Delta\omega_{\text{ref}}|$	step of angular frequency disturbance
ΔP_0	difference of power
s	search direction

This method is achieved by changing the reference value of the frequency by $\Delta\omega_{\text{ref}}$ and then monitoring the corresponding change of the output power, ΔP_0. With an increment (or decrement) of ω_{ref}, the corresponding increment (or decrement) of output power P_0 is estimated. If ΔP_0 is positive with last positive $\Delta\omega_{\text{ref}}$, in per-unit value by $L\Delta\omega_{\text{ref}\ (PU)}$, the search is continued in the same direction. If, on the other hand, *positive* $\Delta\omega_{\text{ref}}$ causes *negative* ΔP_0, the direction of search is reversed. MC achieves maximum wind power acquisition from the WT by driving the angular frequency, ω_e, to its optimal reference value, ω_{ref}. This is accomplished by regulating the active power absorbed by MC, through modulation of phase angle of its SVPWM reference signal as explained in detail in [14, 20].

Figure 12.4 shows the control block diagram of the system that uses the power circuit of Fig. 12.1. The MC uses vector control in inner current control loop to permit fast transient response for system. For a particular wind velocity, there will be an optimum setting of generator speed. The speed loop will generate the torque
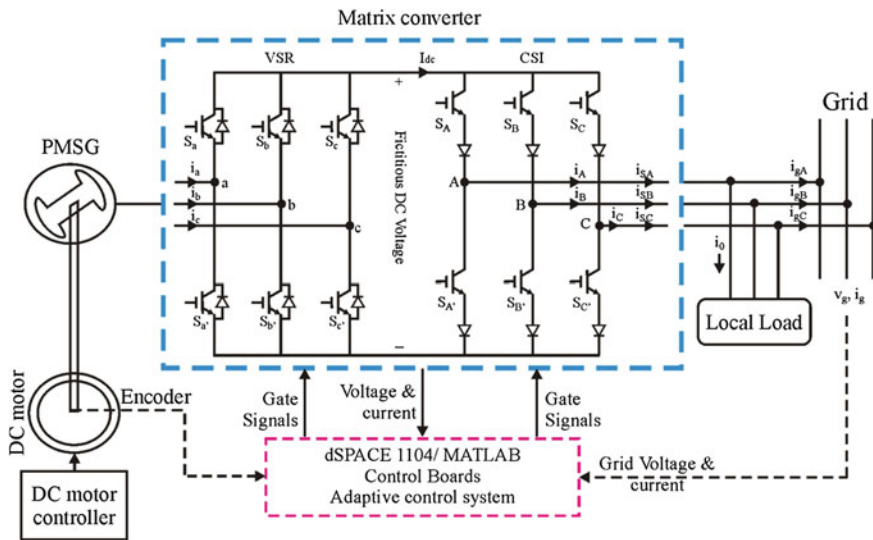
Fig. 12.4 Overall block diagram of the proposed matrix converter-interfaced PMSG for wind energy conversion system

component of machine current so as to balance the developed torque with the load torque [20].

12.4 Development of Hardware Laboratory Prototype

To verify the proposed adaptive control, a laboratory test is carried out on developed 1.2 kW prototype of MC-interfaced PMSG for WECS using dSPACE 1104 real-time control system, which is programmed in the MATLAB/Simulink environment. Figure 12.5 shows the picture of the test rig setup, which is the implementation of block diagram of the proposed system shown in Fig. 12.4. Here, three-phase programmable AC supply is used as a grid. To verify the wind simulator operation, the speed of the shaft is changed by implementing a speed loop control. At different speeds, the input power to the MC is measured. The measured power points are recorded, and the plot of the generator speed versus output power is generated as shown in Fig. 12.6.

Space vector pulse width modulation (SVPWM)-based switching signals given to the switches of MC and dc drive-based WT emulator are presented in Fig. 12.7. Figure 12.8 shows the implementation of space vector modulation (SVM) switching strategy as per explanations in previous section for MC of proposed system in dSPACE 1104 kit in MATLAB/Simulink environment. Three-phase variable resistive load, diode bridge rectifier inverter-fed induction motor, and diode bridge rectifier-fed dc motor are used as nonlinear inductive ac/dc loads.

Fig. 12.5 Schematic of the experimental setup of matrix converter interfaced PMSG for wind energy conversion system
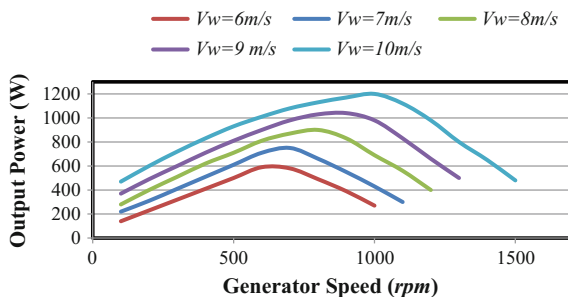

Fig. 12.6 Experimental plot of generator speed versus output power for different wind speeds
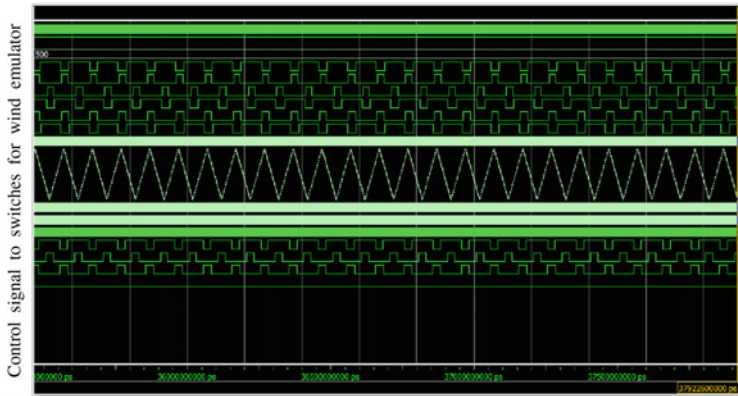
12.5   Experimental Investigation

To verify the adaptive fuzzy control methods for developed laboratory 1.2 kW prototype of MC-based WECS, experimental investigation is carried out under both isolated and grid-connected modes for different balanced/unbalanced load and wind conditions.

(a) Control signal to VSR of MC
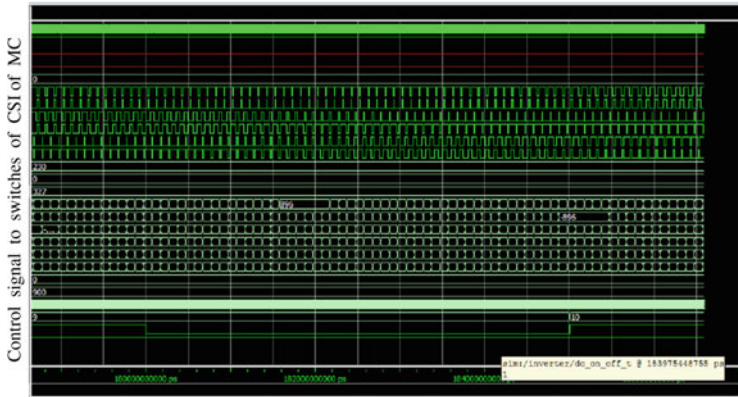
(b) Control signal to CSI of MC

(c) Control signal to dc drive based wind turbine emulator

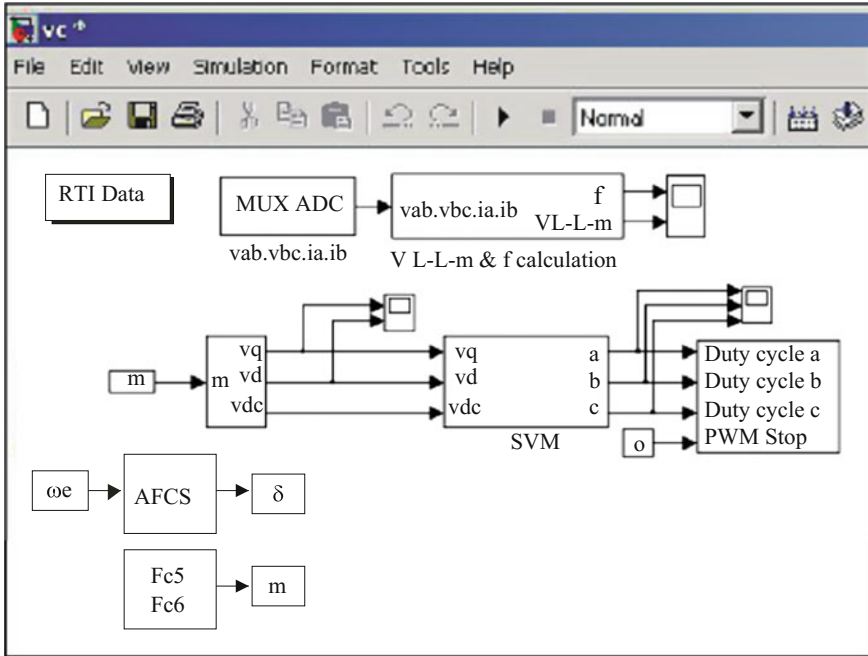**Fig. 12.7** SVPWM switching signals to MC and dc drive-based wind turbine emulator

Fig. 12.8 SVPWM algorithm implemented in dSPACE 1104 for matrix converter of proposed WECS system in MATLAB/Simulink environment

12.5.1   Response Under Isolated Mode

In isolated mode, the main function of the proposed control is to keep the frequency at its set value and to regulate the load voltage at desired level. A certain amount of current corresponding to the rated voltage is fed to the load by the MC to achieve the desired voltage level at load terminals.

12.5.1.1   Response During Constant Resistive and Nonlinear Inductive Load

During isolated mode, WT is controlled to deliver power to an external load through unidirectional indirect MC. Here, the objective of the developed control is to keep regulated voltage across the load. Prototype has been tested experimentally under different resistive and nonlinear inductive load ranging from no load to 2.5 kW at different generator speeds.

From experimental waveforms of Fig. 12.9a, b, it can also be observed that three-phase load current and voltages are properly balanced and well regulated sinusoidally with unity pf for resistive load. Also, it can be seen that phase voltage
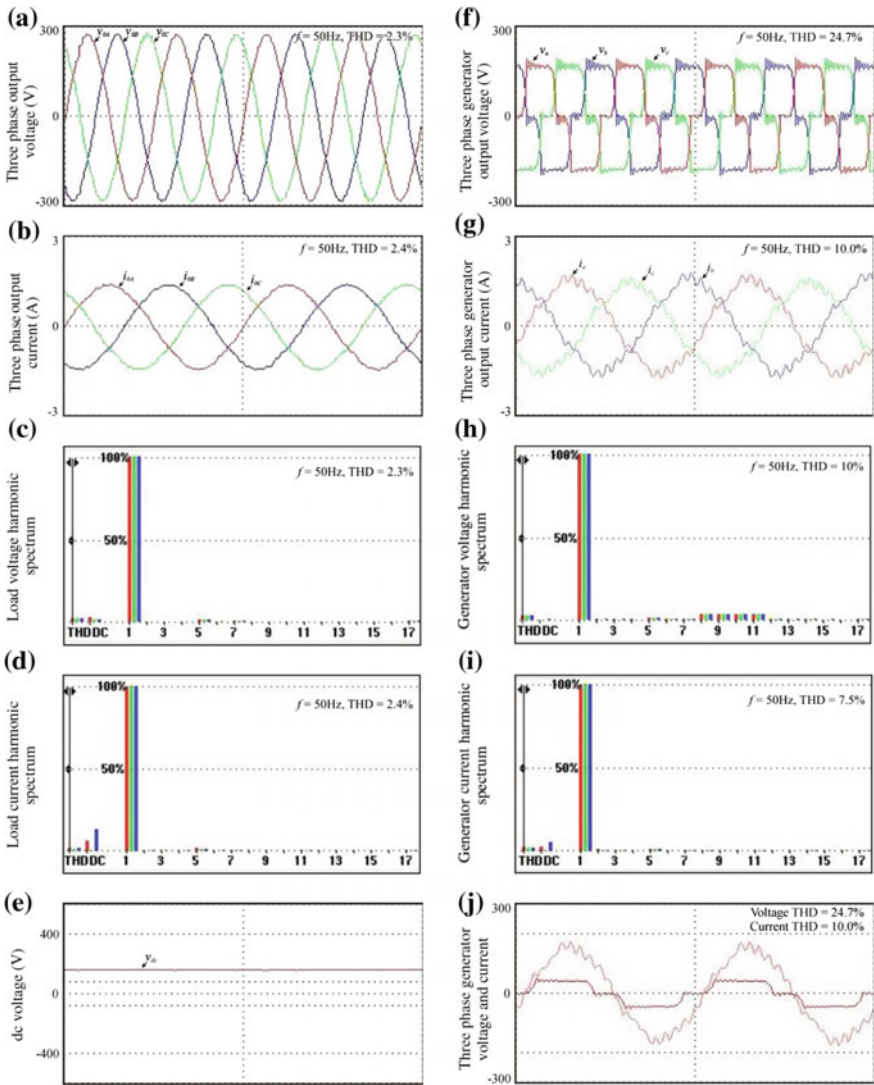
Fig. 12.9 Experimental waveforms during constant resistive load of 1 kW, 1200 rpm:
a three-phase output voltage; **b** three-phase output current; **c** load voltage harmonic spectrum;
d load current harmonic spectrum; **e** fictitious dc link voltage; **f** generator output voltage;
g generator output current; **h** generator voltage harmonic spectrum; **i** generator current harmonic
spectrum; and **j** generator phase voltage and current

and current of generator converter, fictitious dc link voltage, and the load voltage
for resistive load are within safe limits. From load voltage and current harmonic
spectrum of Fig. 12.9c, d, it is shown that total harmonic distortion (THD) of load
voltage and load current is 2.3 and 2.4%, respectively, which is less than 5% and it

is in consent with the permissible limits of IEEE 1547, IEEE 519, and IEC 61727 standards and thus satisfies the general standards of produced power in terms of voltage and current inside 5% THD. Low THD is due to the use of SVPWM switching for the MC.

Unity pf operation with low THD satisfies the pf demand, and is far better as compare to pf and THD of about 0.94 and 4.25%, respectively, in case of converter topology proposed for wind power applications by Ref. [21]. It demonstrates the expected improvement when compared with similar works. Therefore, it is clear that the SVPWM-based MC-interfaced WECS succeeds in regulating the load voltage and frequency within satisfied limits of 220/400 V and 50 Hz, respectively, with low-harmonic characteristics.

12.5.1.2   Response During Nonlinear Inductive Dc Load

In order to validate the developed MC-interfaced WECS, experimental investigation using nonlinear inductive dc load is also carried out.

Here, diode rectifier-fed dc motor is used as a nonlinear inductive dc load. Figure 12.10 presents the experimental waveforms for constant nonlinear inductive dc load of 1 kW at generator speed of 1200 rpm.

12.5.1.3   Response During Varying Load Condition

Figure 12.11 demonstrates the effectiveness of the controls for laboratory prototype of WECS during dynamic conditions. The load is changed from 100 to 50% and then from 50 to 100% to simulate the transient load changing. It is observed that
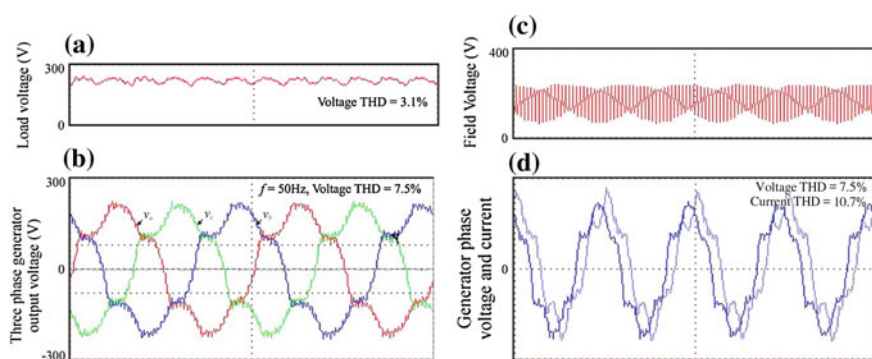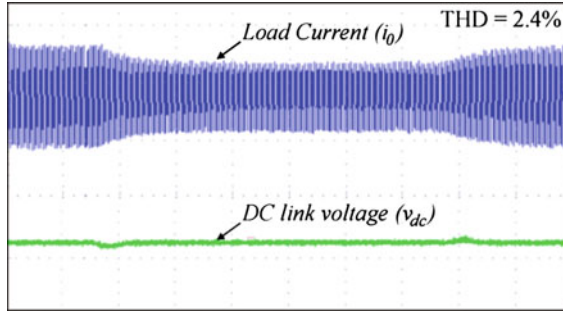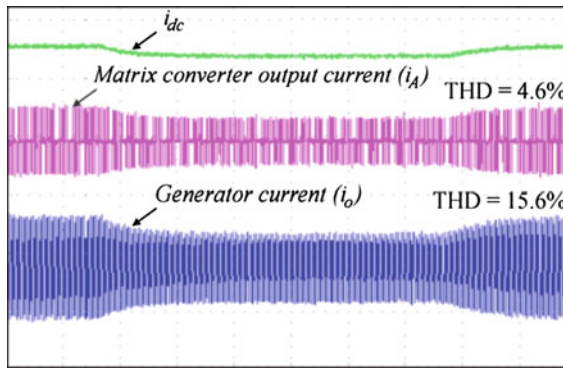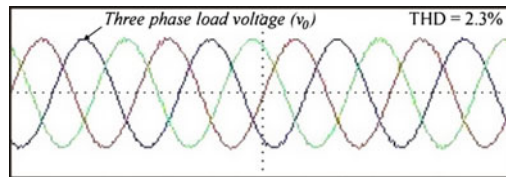

Fig. 12.10 Experimental waveforms during constant nonlinear dc load of 1 A, 1200 rpm: **a** output load voltage; **b** generator output voltage; **c** generator field voltage; and **d** generator phase voltage and current

(a) **Instantaneous load current (i_0), and
fictitious dc link voltage (v_{dc})**

(b) **dc link current (i_{dc}), MC output current
(i_A), and generator current (i_0)**

(c) **Three phase load voltage (v_0)**

Fig. 12.11 Experimental waveform during varying load condition: **a** load voltage and fictitious dc link voltage; **b** dc link current, MC output current, and generator current; **c** three-phase load voltages response when the load changes from 100 to 50% and then from 50 to 100%

load voltage is well maintained despite the variation of loads. But, the load current is changing with load variation as expected.

It is seen that the controller can regulate the load voltage and frequency quite well under varying load conditions. When the load is changed, the load current varies and so closed loop control commands the necessary control action to maintain the constant voltage magnitude.

12.5.2 Response Under Grid-Connected Mode

In grid-connected mode, the main objective of the control algorithm is to track the dispatch power so as to yield maximum energy. Also, to achieve almost unity pf operation at the grid, the reactive power is controlled. Space vector PWM is effectively used to control the MC for interfacing the generator with the grid. Here, in this work, programmable AC supply available in the laboratory is used as a grid.

12.5.2.1 Under Steady-State Condition

The steady-state grid phase voltage and current waveforms for unity, lagging, and leading pf operations are shown in Fig. 12.12a–c.

This demonstrates the reactive power capability of the MC for wind power applications. The reactive power control capability of the proposed MC-based WECS is also illustrated in Fig. 12.12d for unity, lagging, and leading pf operation,
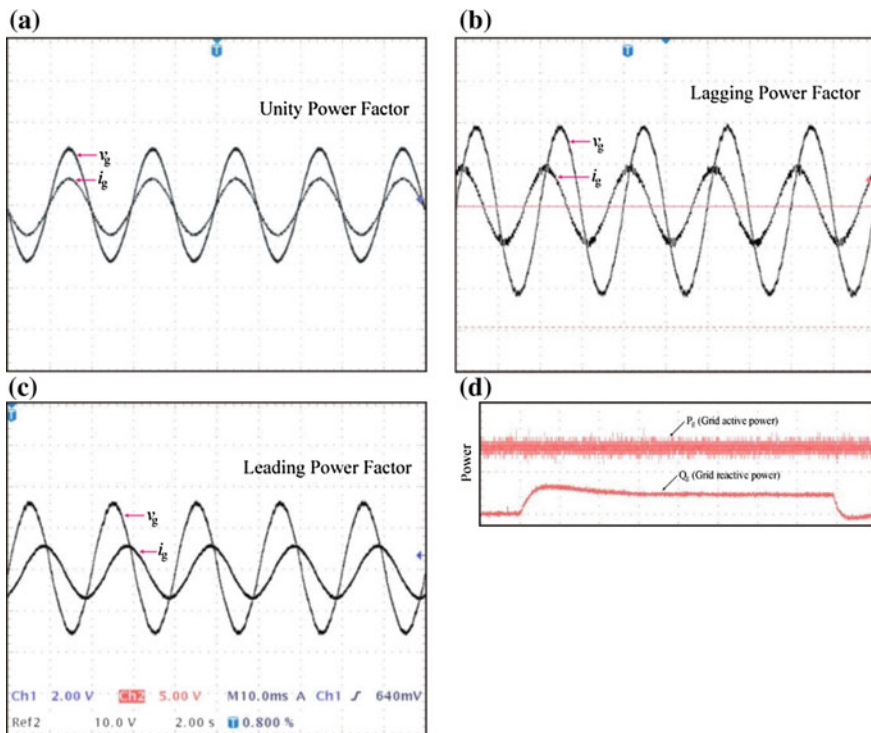

Fig. 12.12 Steady state grid phase voltage v_g and injected grid current i_g waveforms for **a** unity power factor operation; **b** lagging power factor operation; **c** leading power factor operation; and **d** injected grid active power P_g and reactive power Q_g
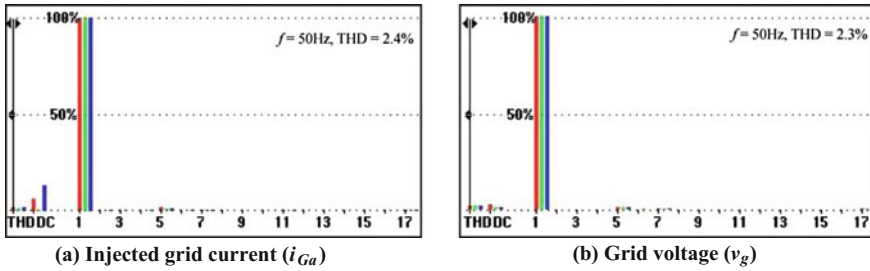
Fig. 12.13 Harmonic spectrum for injected grid current (i_{gA}) and grid voltage (v_g)

while keeping active power constant. Figure 12.12 shows the experimental results during steady-state condition. From experimental waveform of Fig. 12.12a, it is shown that grid phase voltage is regulated and sinusoidal, whereas that of dc link voltage is almost dc without any distortion. It can be observed from Fig. 12.12b that grid-injected phase current and voltages are well regulated sinusoidally with almost unity pf. A good equilibrium among the voltages can be seen. Also, the unfiltered MC current (i_A) is in phase with the grid phase voltage (v_g).

The grid current (i_g) has a slight phase lag induced by the filter capacitor, but this phase lag is negligible when the MC's current injection into the grid is increased. Figure 12.12c shows three-phase output grid currents illustrating the balanced nature. Figure 12.13 presents the harmonic spectrum for injected grid current and voltage, where it can be seen that THD is 2.4 and 2.3%, respectively. Also, pf is equal to 0.996 and THD is about 2.3%, which satisfies the pf demand, and is far better as compared to pf and THD of about 0.94 and 4.25%, respectively, in case of converter topology proposed for wind power applications in [21].

The THD measured for grid-injected current and voltage is quite low as per standard IEEE 1547, IEEE-519, and IEC 61727 and thus satisfies the general standards of produced power in terms of voltage and current THDs within the limits of 5%. This improvement in pf results in the reduction of about 13% generator conduction losses. This demonstrates the expected improvement when compared with similar works by [6, 21–23]. It is clear that this proposed optimal controller for MC interfaced WECS succeeds in regulating the load voltage and frequency within limits of 220/400 V and 50 Hz, respectively.

12.5.2.2 Dynamic Response Under Change in Current Command

To validate the robustness of voltage boost function of the MC, proposed system dynamic response is tested experimentally when current commands are increased and decreased. Figure 12.14 verifies the effectiveness of the proposed

Fig. 12.14 Experimental waveforms during change in MC current command. **a** MC input current (i_a) and grid currents (i_{gA} and i_{gB}) response of current command decreasing; **b** MC input current (i_a) and grid currents (i_{gA} and i_{gB}) response of current command increasing; and **c** three-phase grid voltages (v_{gA}, v_{gB}, v_{gC}) during change in current command
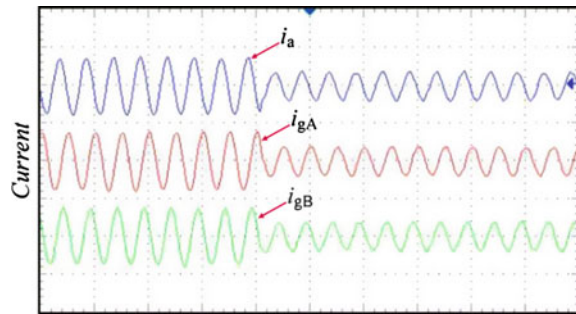
(a) Current command decreasing
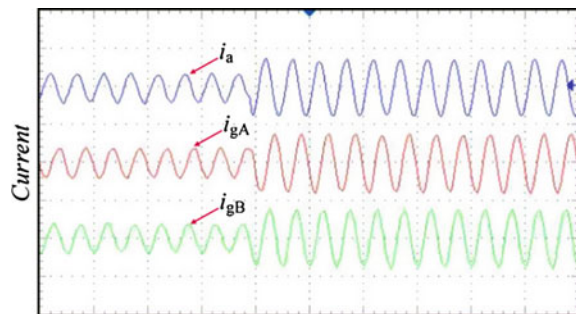
(b) Current command increasing
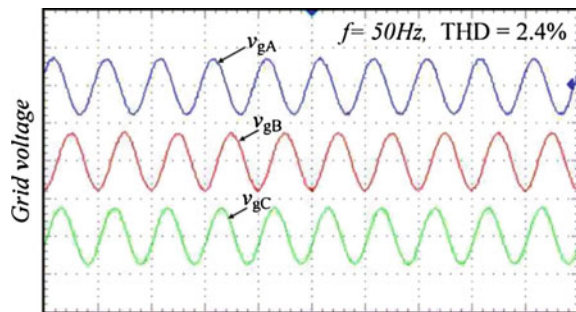
(c) Three phase grid voltages (v_{gA}, v_{gB}, v_{gC})

high-efficiency control system of the MC-interfaced WECS when input current amplitude commands are decreased from 3.5 to 1.5 A and increased from 1.5 to 3.5 A, respectively.

It can be noticed from the experimental waveforms that unity pf is maintained, despite of dynamic current command changing. Also, input current of MC can track effectively its current commands. The output current increases or decreases accordingly without deteriorating waveforms.

12.6   Conclusion

This chapter presents detailed explanation of the application and development of MC for DG. It also presents the experimental investigation of merits and demerits of use of MC for wind power application. From the experimental results, it can be verified that a good equilibrium among the load currents and voltages can be seen. Also, the load voltage and current waveforms are properly balanced and well regulated sinusoidally with unity pf operation for resistive load. Also, THD of load voltage and load current is 2.3 and 2.4%, respectively, which is less than 5% and it is in consent with the permissible limits of IEEE standard 1547, IEEE 519, and IEC 61727 and thus satisfies the general standards of produced power in terms of voltage and current inside 5%. Low THD is due to the use of SVPWM switching for the MC. This improvement in pf results in the reduction of about 13% in generator conduction losses.

References

1. Freries LL (1990) Wind energy conversion systems. Prentice Hall, New York
2. Ackermann LST (2000) Wind Energy technology and current status: a review. Renew Sustain Energy Rev 4:315–375
3. Bansal RC, Zobaa AF, Saket RK (2005) Some issues related to power generation using wind energy conversion systems: an overview. Int J Emerg Electr Power Syst 3(2):1–19
4. Hansen AD, Iov F, Blaabjerg F, Hansen LH (2011) Review of contemporary wind turbine concepts and their market penetration. J Wind Eng 58(4):1081–1095
5. Liserre M, Cardenas M, Molinas M, Rodriguez J (2011) Overview of multi-MW wind turbines and wind parks. IEEE Trans Ind Electron 58(4):1081–1095
6. Chinchilla M, Arnaltes S, Burgos (2006) Control of permanent-magnet generators applied to variable-speed wind-energy systems connected to the grid. IEEE Trans Energy Convers 21 (1):130–135
7. Kim KH, Jeung YC, Lee DC, Kim HG (2011) LVRT scheme of PMSG wind power systems based on feedback linearization. IEEE Trans Power Electron 27(5):2376–2384
8. Ma K, Blaabjerg M (2012) The impact of power switching devices on the thermal performance of a 10 MW wind power NPC converter. Energies 5(7):2559–2577
9. Blaabjerg F, Liserre M, Ma K (2012) Power electronics converters for wind turbine systems. IEEE Trans Ind Appl 48(2):708–719
10. Amei K, Takayasu Y, Ohji T, Sakui M (2002) A maximum power control of wind generator system using a permanent magnet synchronous generator and a boost chopper circuit. In: Proceeding of PCC, pp 1447–1452
11. Peña R, Cárdenas R, Reyes E, Clare J, Wheeler P (2009) A topology for multiple generation system with doubly fed induction machines and indirect matrix converter. IEEE Trans Ind Electron 56(10):4181–4193
12. Naidu M, Walters J (2003) A 4-kW 42-V induction-machine-based automotive power generation system with a diode bridge rectifier and a PWM inverter. IEEE Trans Ind Appl 39 (5):1287–1293
13. Teodorescu R, Blaabjerg F (2004) Flexible control of small wind turbines with grid failure detection operating in stand-alone and grid connected mode. IEEE Trans Power Electron 19 (5):1323–1332

14. Kumar V, Joshi RR, Bansal RC (2009) Optimal control of matrix converter based WECS for performance enhancement and efficiency optimization. IEEE Trans Energy Conver 24 (1):264–273
15. Tazil M, Kumar V, Bansal RC, Kong S, Dong ZY, Freitas W, Mathur HD (2010) Three-phase doubly-fed induction generators: an overview. IET Electr Power Appl 4(2):75–89
16. Liu X, Wang P, Loh PC, Blaabjerg F (2011) A Three-phase dual-input matrix converter for grid integration of two ac type energy resources. IEEE Trans Ind Electron 60(1):20–30
17. Barakati SM, Kazerani M, Aplevich JD (2009) Maximum power tracking control for a wind turbine system including a matrix converter. IEEE Trans Energy Convers 24(3):705–713
18. Ghedamsi K, Aouzellag D, Berkouk EM (2006) Application of matrix converter for variable speed wind turbine driving a doubly fed induction generator. In: Proceedings of IEEE international symposium on power electronics, electrical drives, automation and motion, pp 1201–1205
19. Cardenas R, Pena R, Tobar G, Clare J, Wheeler P, Asher G (2009) Stability analysis of a wind energy conversion system based on a doubly fed induction generator fed by a matrix converter. IEEE Trans Ind Electron 56(10):4194–4206
20. Kumar V, Joshi RR, Bansal RC (2015) Development of a novel control for matrix converter interfaced wind energy conversion system for dynamic performance enhancement. Taylor Francis J Electr Compon Power Syst 43(8–10):1062–1071
21. Oliveira DS, Reis JM, Silva CEA, Barreto LH, Fernando LM, Bruno LS (2010) A three-phase high-frequency semicontrolled rectifier for PM WECS. IEEE Trans Power Electron 25 (3):677–685
22. Haque ME, Negnevitsky M, Muttaqi KM (2010) A novel control strategy for a variable-speed wind turbine with a permanent-magnet synchronous generator. IEEE Trans Ind Appl 46 (1):331–339
23. Karaman E, Farasat M, Trzynadlowski AM (2013) Permanent-magnet synchronous-generator wind-energy systems with boost matrix converters. In: Proceeding of IEEE energy conversion congress and exposition, pp 2977–2981